Stochastic analysis of an epidemic SVIR model with Holling type II incidence and treatment rates

M N Srinivas[1], M. Lakshmi[2], V. Kamalakannan[3] V Madhusudanan[4]

[1]Department of Mathematics, School of Advanced Sciences,
Vellore Institute of Technology, Vellore 632014, Tamil Nadu, India
E-mail:mnsrinivaselr@gmail.com

[2] Department of Mathematics, S.A. Engineering College,
Chennai 600077, Tamil Nadu, India
E-mail: lakshmim@saec.ac.in

[3]Department of Mathematics, Panimalar. Engineering College,
Chennai 600123, Tamil Nadu, India
E-mail: mail2kamalakannan@gmail.com

[4*] Department of Mathematics, S.A. Engineering College,
Chennai 600077, Tamil Nadu, India
E-mail: mvms.maths@gmail.com

Abstract

In the event of an epidemic, inhibitory effects play a critical role in limiting the pandemic's influence on society. The majority of infectious diseases that affect humans are still on the verge of becoming epidemics over the world. Mathematical models have long been used to investigate the complicated dynamics of infectious illnesses. This research investigates a stochastic SVIR epidemic model with Holling type II incidence and treatment rates. The Fourier transform approach is used to analyse stochastic stability around an internal steady state. Finally, numerical simulations are presented with appropriate parameter selections in order to test the efficiency of the theoretical results.

Keywords: Holling type II treatment rate, incidence rate, SVIR model, epidemiology, Fourier transform

1. Introduction

Many infectious diseases are common and prevalent, posing a serious concern for healthcare workers and politicians around the world. In recent years, controlling infectious diseases has become a more difficult task. A comprehensive grasp of the mechanics of a disease's progression is essential to control or eliminate it. Epidemiologists [1–13] have attempted to create mathematical models based on the observed characteristics of infectious diseases in

order to comprehend various features of many diseases and recommend techniques for their control. The manner in which an infectious disease is transmitted is a critical consideration in the research of its transmission. The incidence rate, defined as the average number of new cases of a disease per unit period in epidemiology, determines the transmission of an infectious disease. As a result, the incidence rate is critical in the study of the qualitative description of infectious disease transmission dynamics. Many scholars [14–17] developed nonlinear transmission laws to examine the dynamics of infectious diseases, such as the Holling type II functional, Crowley–Martin functional, Beddington–DeAngelis functional, and others.

Even in the face of catastrophic disasters, humans continue to progress. Throughout history, many significant infectious diseases have killed a large number of people, and the number of people killed is far more than the number of people killed in world wars. According to World Health Statistics 2019, infectious illnesses still account for six of the top ten causes of mortality in low-income countries, including malaria, tuberculosis, and HIV [18]. In 2018, HIV, TB, and malaria caused 0.8, 1.2, and 0.4 million fatalities, respectively, according to World Health Statistics 2020 [19]. As a result, it is critical that the government and professionals take the required steps to study and limit infectious illness spread. Daniel Bernoulli, a great mathematician, utilised differential equations to assess the availability of variation in healthy humans infected with the smallpox virus as early as 1760. Since Daniel Bernoulli's groundbreaking discovery, other epidemic models have been constructed to research and study the spread law of infectious illnesses. For instance, the SIS [20-22], SIR [23-27], SEIS [28-31], SEIR [32-35] , SEIRS [36–38] epidemic models, and various other models involving vaccination [39–42] and quarantine [43-44]. Goel et al. [45] suggested a time-delayed SVIRS epidemic model to examine the influence of saturated incidence and saturated therapy and in the proposed system, they looked at local stability and the occurrence of Hopf bifurcation. Also, Zizhen Zhang et al. [46] proposed a deterministic SVIRS epidemic model with Holling type II incidence and treatment rates, as well as three delays and examined the dynamics. Hopf bifurcation and the local stability of disease equilibrium are thoroughly described. The direction and stability of bifurcated periodic solutions are then determined.

This work is coordinated as follows. In Section 2, we figure the numerical model of our concern. Segment 3 gives the elements of the model without noise. Segment 4 furnishes the elements of the model with noise. Dissemination examination of the numerical model is talked about in segment 5. Computational recreations are acted in Section 6. In the last segment, Section 7, we close and give a few comments and future works.

2. Mathematical model with noise:

In this section, we considered a SVIR stochastic epidemic model in which we are considering four compartments like susceptible, vaccinated, infected and recovered with Holling type II

incidence rate, treatment rate by the motivation of [46]. Specifically we are investigating the effect of Gaussian white noise on the model (without delay) proposed by Zizhen Zhang et.al [46] for various low, medium and high intensities. The schematic representation of the proposed model is as follows.

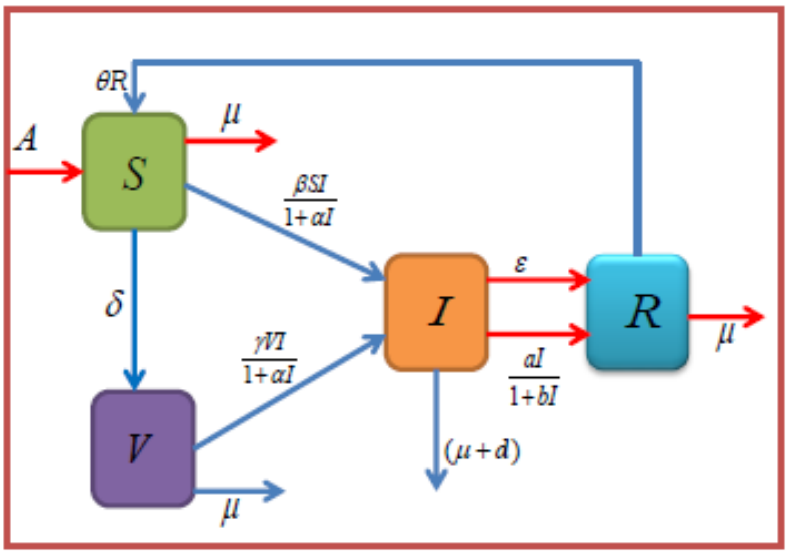

Figure (H)

Figure (H) represents schematic representation of SVIR model system

The following system of nonlinear differential equations with noise describes the dynamics of the proposed model.

$$S'(t) = A - \delta S - \frac{\beta SI}{1+\alpha I} - \mu S + \theta R + \alpha_1 \xi_1(t) \tag{2.1}$$

$$V'(t) = \delta S - \frac{\gamma VI}{1+\alpha I} - \mu V + \alpha_2 \xi_2(t) \tag{2.2}$$

$$I'(t) = \frac{\beta SI}{1+\alpha I} + \frac{\gamma VI}{1+\alpha I} - (\mu + d) I - \varepsilon I - \frac{aI}{1+bI} + \alpha_3 \xi_3(t) \tag{2.3}$$

$$R'(t) = \varepsilon I + \frac{aI}{1+bI} - \theta R - \mu R + \alpha_4 \xi_4(t) \tag{2.4}$$

where $S(t)$, $V(t)$, $I(t)$ and $R(t)$ represent numbers of susceptible, vaccinated, infective and recovered at time t, respectively. A represents the rate at which susceptible individuals become infected, β represents the force of infection, α represents the infected inhibition measures, γ represents the rate at which people who have been immunised become infected, δ shows the proportion of vaccinated people who become infected and infected people who

become infected, and θ reflects the rate of transfer from recovered to susceptible people, ε is the rate at which infected people become infected again, μ is the average natural mortality rate of all people d is the disease-related death rate, a is the rate of treatment, and b is the rate at which medical resources are scarce.

3. Dynamical behaviour without noise

By the motivation of [45] and [46], we are studying the effect of noise on the SVIR disease system (2.1-2.4). In this process, we are adopting some observations done by [46] in this section without additive white noise.

The majority of infectious diseases that affect humans are still on the verge of becoming epidemics over the world. Mathematical models have long been used to investigate the complicated dynamics of infectious illnesses. The researchers [46] looked at a three-delay deterministic SVIRS epidemic model with a Holling type II incidence and treatment rates. Hopf bifurcation and the local stability of disease equilibrium are thoroughly described. The bifurcated periodic solution's direction and stability are then determined. Finally, numerical simulations with appropriate parameter selections are presented in order to assess the efficacy of the theoretical results obtained.

4. Dynamical behaviour with noise

Ecological systems are characterised by a number of forces that are not constant in time but change, such as climate and natural disturbances. Due to the uncertainty inherent in weather patterns, climate fluctuations, and episodic disturbances such as earthquakes, landslides, fires, insect outbreaks, and so on, a significant portion of environmental variability is random, with the exception of processes dominated by deterministic oscillations. The existence of random drivers in bio-geophysical processes motivates the study of how a stochastic environment might alter and characterise the dynamics of natural systems. Now we'll look at the stochastic models (2.1)-(2.4) to see how random environmental variations affect stability. The model's parameters swing around their average values due to random variations. With additive white noises, we consider the randomness of the model (2.1)-(2.4). The white noise perturbation will modify any model parameter ν as $\nu+\alpha\xi(t)$, where α is the noise amplitude and $\xi(t)$ is a Gaussian white noise process at time t. The deterministic and stochastic models, on the other hand, have the identical equilibrium states, which will now vary around their mean states.

In this analysis, we emphasis on the dynamics of the model (2.1)-(2.4) about the interior equilibrium point $\tilde{E}\left(S^*,V^*,I^*,R^*\right)$ only according to the method introduced by Nisbet and Gurney [47] , Carletti [48] and motivated by [49-53].

Let $S(t)=u_1(t)+S^*;\ V(t)=u_2(t)+V^*;\ I(t)=u_3(t)+I^*;\ R(t)=u_4(t)+R^*;$ (4.1)

and by focusing solely on the effects of linear stochastic perturbations As a result, the model (2.1)-(2.4) is reduced to the linear system shown below.

$$u_1'(t) = -\beta S^* u_3 + \alpha_1 \xi_1(t) \tag{4.2}$$

$$u_2'(t) = \alpha_2 \xi_2(t) \tag{4.3}$$

$$u_3'(t) = \beta I^* u_1 + \gamma I^* u_2 + \alpha_3 \xi_3(t) \tag{4.4}$$

$$u_4' = \alpha_4 \xi_4(t) \tag{4.5}$$

Taking the Fourier transform of (4.2) - (4.5) we get,

$$\alpha_1 \tilde{\xi}_1(\omega) = (i\omega)\tilde{u}_1(\omega) + \left(\beta S^*\right)\tilde{u}_3(\omega) \tag{4.6}$$

$$\alpha_2 \tilde{\xi}_2(\omega) = (i\omega)\tilde{u}_2(\omega) \tag{4.7}$$

$$\alpha_3 \tilde{\xi}_3(\omega) = \left(-\beta I^*\right)\tilde{u}_1(\omega) + \left(\gamma I^*\right)\tilde{u}_2(\omega) + (i\omega)\tilde{u}_3(\omega) \tag{4.8}$$

$$\alpha_4 \tilde{\xi}_4(\omega) = (i\omega)\tilde{u}_4(\omega) \tag{4.9}$$

Equations (4.6) and (4.9) have a matrix form as

$$M(\omega)\tilde{u}(\omega) = \tilde{\psi}(\omega) \tag{4.10}$$

where, $M(\omega) = \begin{pmatrix} A_1 & B_1 & C_1 & D_1 \\ A_2 & B_2 & C_2 & D_2 \\ A_3 & B_3 & C_3 & D_3 \\ A_4 & B_4 & C_4 & D_4 \end{pmatrix}$;

$\tilde{u}(\omega) = \left[\tilde{u}_1(\omega), \tilde{u}_2(\omega), \tilde{u}_3(\omega), \tilde{u}_4(\omega)\right]^T$;

$\tilde{\xi}(\omega) = \left[\alpha_1 \tilde{\xi}_1(\omega), \alpha_2 \tilde{\xi}_2(\omega), \alpha_3 \tilde{\xi}_3(\omega), \alpha_4 \tilde{\xi}_4(\omega)\right]^T$;

$A_1 = i\omega$; $B_1 = 0$; $C_1 = \beta S^*$; $D_1 = 0$; $A_2 = 0$; $B_2 = i\omega$; $C_2 = 0$; $D_2 = 0$;

$A_3 = -\beta I^*$; $B_3 = -\gamma I^*$; $C_3 = i\omega$; $D_3 = 0$; $A_4 = 0$; $B_4 = 0$; $C_4 = 0$; $D_4 = i\omega$;

Alternatively, equation (4.10) can be written as

$$\tilde{u}(\omega) = \left[M(\omega)\right]^{-1} \tilde{\xi}(\omega) \tag{4.11}$$

Let $\left[M(\omega)\right]^{-1} = K(\omega)$ (4.12)

where $K(\omega) = \dfrac{adj\left[M(\omega)\right]}{\left|M(\omega)\right|}$ (4.13)

If the function's $Y(t)$ mean value is zero, the fluctuation intensity (variance) of its components in frequency intervals $[\omega, \omega + d\omega]$ is $S_Y(\omega)d\omega$, where $S_Y(\omega)$ is the spectral density Y and is defined as

$$S_y(\omega) = \lim_{\tilde{T}\to+\infty} \frac{\left|Y(\omega)\right|^2}{\tilde{T}} \tag{4.14}$$

The auto covariance function is the inverse transform of $S_Y(\omega)$ if Y has a zero mean value.

$$C_Y(\tau) = \frac{1}{2\pi}\int_{-\infty}^{\infty} S_Y(\omega) e^{i\omega\tau}\, d\omega \tag{4.15}$$

and the variance of the corresponding fluctuations in $Y(t)$ is given by

$$\sigma_Y{}^2 = C_Y(0) = \frac{1}{2\pi}\int_{-\infty}^{\infty} S_Y(\omega)\, d\omega \tag{4.16}$$

The normalised auto covariance function is the auto correlation function.

$$P_Y(\tau) = \frac{C_Y(\tau)}{C_Y(0)} \tag{4.17}$$

For a Gaussian white noise process, it is

$$S_{\xi_i,\xi_j}(\omega) = \lim_{\tilde{T}\to\infty}\left[\frac{E\left[\tilde{\xi}_i(\omega), \tilde{\xi}_j(\omega)\right]}{\tilde{T}}\right] \tag{4.18}$$

$$= \lim_{\tilde{T}\to\infty}\frac{1}{\tilde{T}}\int_{-\tilde{T}/2}^{\tilde{T}/2}\int_{-\tilde{T}/2}^{\tilde{T}/2} E\left[\xi_i(t), \xi_j(t')\right] e^{-i\omega(t-t')} dt\, dt' = \delta_{ij} \tag{4.19}$$

The components of (4.11)'s solutions are as follows:

$$\tilde{u}_i(\omega) = \sum_{j=1}^{4} K_{ij}(\omega)\tilde{\xi}_j(\omega);\ i = 1,2,3,4 \tag{4.20}$$

The range of u_i, $i = 1,2,3,4$ is provided by

$$S_{u_i}(\omega)=\sum_{j=1}^{4}\alpha_j\left|K_{ij}(\omega)\right|^2;\ i=1,2,3,4 \tag{4.21}$$

Hence the intensities of fluctuations in the variable u_i, $i=1,2,3,4$ are given by

As a result, the intensities of the variable's u_i, $i=1,2,3,4$ fluctuations are given by

$$\sigma_{u_i}{}^2=\frac{1}{2\pi}\sum_{j=1}^{4}\int_{-\infty}^{\infty}\alpha_j\left|K_{ij}(\omega)\right|^2 d\omega;\ i=1,2,3,4 \tag{4.22}$$

In other words, the variances of u_i, $i=1,2,3,4$ are calculated as

$$\sigma_{u_1}{}^2=\frac{1}{2\pi}\left\{\int_{-\infty}^{\infty}\alpha_1\left|\frac{A_{11}(\omega)}{|M(\omega)|}\right|^2 d\omega+\int_{-\infty}^{\infty}\alpha_2\left|\frac{A_{12}(\omega)}{|M(\omega)|}\right|^2 d\omega+\int_{-\infty}^{\infty}\alpha_3\left|\frac{A_{13}(\omega)}{|M(\omega)|}\right|^2 d\omega+\int_{-\infty}^{\infty}\alpha_4\left|\frac{A_{14}(\omega)}{|M(\omega)|}\right|^2 d\omega\right\}$$

$$\sigma_{u_1}{}^2=\frac{1}{2\pi}\left\{\int_{-\infty}^{\infty}\alpha_1\left|\frac{B_{11}(\omega)}{|M(\omega)|}\right|^2 d\omega+\int_{-\infty}^{\infty}\alpha_2\left|\frac{B_{12}(\omega)}{|M(\omega)|}\right|^2 d\omega+\int_{-\infty}^{\infty}\alpha_3\left|\frac{B_{13}(\omega)}{|M(\omega)|}\right|^2 d\omega+\int_{-\infty}^{\infty}\alpha_4\left|\frac{B_{14}(\omega)}{|M(\omega)|}\right|^2 d\omega\right\}$$

$$\sigma_{u_1}{}^2=\frac{1}{2\pi}\left\{\int_{-\infty}^{\infty}\alpha_1\left|\frac{C_{11}(\omega)}{|M(\omega)|}\right|^2 d\omega+\int_{-\infty}^{\infty}\alpha_2\left|\frac{C_{12}(\omega)}{|M(\omega)|}\right|^2 d\omega+\int_{-\infty}^{\infty}\alpha_3\left|\frac{C_{13}(\omega)}{|M(\omega)|}\right|^2 d\omega+\int_{-\infty}^{\infty}\alpha_4\left|\frac{C_{14}(\omega)}{|M(\omega)|}\right|^2 d\omega\right\}$$

$$\sigma_{u_1}{}^2=\frac{1}{2\pi}\left\{\int_{-\infty}^{\infty}\alpha_1\left|\frac{D_{11}(\omega)}{|M(\omega)|}\right|^2 d\omega+\int_{-\infty}^{\infty}\alpha_2\left|\frac{D_{12}(\omega)}{|M(\omega)|}\right|^2 d\omega+\int_{-\infty}^{\infty}\alpha_3\left|\frac{D_{13}(\omega)}{|M(\omega)|}\right|^2 d\omega+\int_{-\infty}^{\infty}\alpha_4\left|\frac{D_{14}(\omega)}{|M(\omega)|}\right|^2 d\omega\right\} \tag{4.23}$$

Here $M(\omega)=R(\omega)+iI(\omega)$, where $R(\omega)$ is the real part of $M(\omega)$ and $I(\omega)$ is the an imaginary part of $M(\omega)$, $|M(\omega)|^2=[R(\omega)]^2+[I(\omega)]^2$

$A_{11}=-i\omega^3;\ A_{12}=-\beta\gamma S^*I^*;\ A_{13}=\omega^2\beta S^*;\ A_{14}=0;\ B_{11}=0;\ B_{12}=-i\omega^3+i\omega\beta^2S^*I^*;$
$B_{13}=0;B_{14}=0;C_{14}=-\omega^2\beta I^*;C_{12}=-\omega^2\gamma I^*;C_{13}=-i\omega^3;C_{14}=0;\ D_{11}=0;\ D_{12}=0;\ D_{13}=0;$
$D_{14}=-i\omega^3+i\omega\beta^2S^*I^*;$

We can derive the following from these numbers and equation (4.23):

$$\sigma_{u_1}{}^2=\frac{1}{2\pi}\int_{-\infty}^{\infty}\frac{1}{(\omega^4-\beta^2\omega^2I^*S^*)}\left[\alpha_1(-\omega^3)^2+\alpha_2(-\beta\gamma S^*I^*)^2+\alpha_3(\omega^2\beta S^*)^2\right]d\omega \tag{4.24}$$

$$\sigma_{u_2}{}^2=\frac{1}{2\pi}\int_{-\infty}^{\infty}\frac{1}{(\omega^4-\beta^2\omega^2I^*S^*)}\left[\alpha_2(-\omega^3+\omega\beta^2\gamma S^*I^*)^2\right]d\omega \tag{4.25}$$

$$\sigma_{u_1}{}^2 = \frac{1}{2\pi}\int_{-\infty}^{\infty} \frac{1}{(\omega^4 - \beta^2\omega^2 I^* S^*)}\left[\alpha_1(-\omega^2\beta I^*)^2 + \alpha_2(-\omega^2\gamma I^*)^2 + \alpha_3(-i\omega^3)^2\right]d\omega \tag{4.26}$$

$$\sigma_{u_1}{}^2 = \frac{1}{2\pi}\int_{-\infty}^{\infty} \frac{1}{(\omega^4 - \beta^2\omega^2 I^* S^*)}\left[\alpha_4(-\omega^3 + \omega\beta^2 S^* I^*)^2\right]d\omega \tag{4.27}$$

If we're interested in the system dynamics of (4.1)-(4.4) with either $\alpha_1 = 0$ (or) $\alpha_2 = 0$ (or) $\alpha_3 = 0$ (or) $\alpha_4 = 0$, then the population variances are

If $\alpha_1 = \alpha_2 = \alpha_3 = 0$ then,

$$\sigma_{u_1}{}^2 = \sigma_{u_2}{}^2 = \sigma_{u_3}{}^2 = 0;$$

$$\sigma_{u_4}{}^2 = \frac{\alpha_1}{2\pi}\int_{-\infty}^{\infty} \frac{(-\omega^3 + \omega\beta^2 S^* I^*)^2}{\omega^4 - \beta^2\omega^2 S^* I^*}\,d\omega;$$

If $\alpha_1 = \alpha_3 = \alpha_4 = 0$ then,

$$\sigma_{u_1}{}^2 = \frac{\alpha_2}{2\pi}\int_{-\infty}^{\infty} \frac{(-\beta\gamma S^* I^*)^2}{\omega^4 - \beta^2\omega^2 S^* I^*}\,d\omega;$$

$$\sigma_{u_2}{}^2 = \frac{\alpha_2}{2\pi}\int_{-\infty}^{\infty} \frac{(-\omega^3 + \omega\beta^2 S^* I^*)^2}{\omega^4 - \beta^2\omega^2 S^* I^*}\,d\omega;$$

$$\sigma_{u_3}{}^2 = \frac{\alpha_2}{2\pi}\int_{-\infty}^{\infty} \frac{(-\omega^2\gamma I^*)^2}{\omega^4 - \beta^2\omega^2 S^* I^*}\,d\omega;$$

$$\sigma_{u_4}{}^2 = 0;$$

If $\alpha_1 = \alpha_2 = \alpha_4 = 0$ then,

$$\sigma_{u_1}{}^2 = \frac{\alpha_3}{2\pi}\int_{-\infty}^{\infty} \frac{(\omega^2\beta S^*)^2}{\omega^4 - \beta^2\omega^2 S^* I^*}\,d\omega; \qquad \sigma_{u_2}{}^2 = 0;$$

$$\sigma_{u_3}{}^2 = \frac{\alpha_3}{2\pi}\int_{-\infty}^{\infty} \frac{(-i\omega^3)^2}{\omega^4 - \beta^2\omega^2 S^* I^*}\,d\omega; \qquad \sigma_{u_4}{}^2 = 0;$$

If $\alpha_2 = \alpha_3 = \alpha_4 = 0$ then,

$$\sigma_{u_1}{}^2 = \frac{\alpha_1}{2\pi}\int_{-\infty}^{\infty}\frac{(-\omega^3)^2}{\omega^4-\beta^2\omega^2 S^* I^*}d\omega; \qquad \sigma_{u_2}{}^2 = 0;$$

$$\sigma_{u_3}{}^2 = \frac{\alpha_1}{2\pi}\int_{-\infty}^{\infty}\frac{(-\omega^2\beta I^*)^2}{\omega^4-\beta^2\omega^2 S^* I^*}d\omega; \qquad \sigma_{u_4}{}^2 = 0;$$

Thus, for modest levels of mean square fluctuations, population variances imply population stability, whereas larger values of population variances suggest population instability.

5. Numerical simulations

Example1: For the parameters $A=12;\ \alpha=0.15;\ \beta=0.05;\ \gamma=0.01;\ a=2;\ b=10;\ \theta=0.2;$ $\varepsilon=0.2;\ \alpha_1=0.01;\ \alpha_2=0.02;\ \alpha_3=0.01;\ \alpha_4=0.02$ with initial values [12, 10, 8, 5]

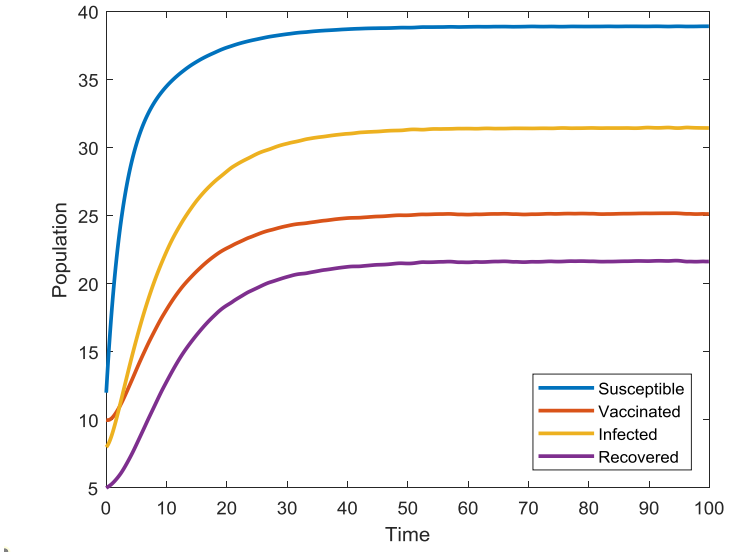

Figure 1

Figure 1 represents time series evaluation of population for the values of the attributes of example 1 with noise intensities $\alpha_1=0.01;\ \alpha_2=0.02;\ \alpha_3=0.01;\ \alpha_4=0.02$ and with initial values [12, 10, 8, 5]

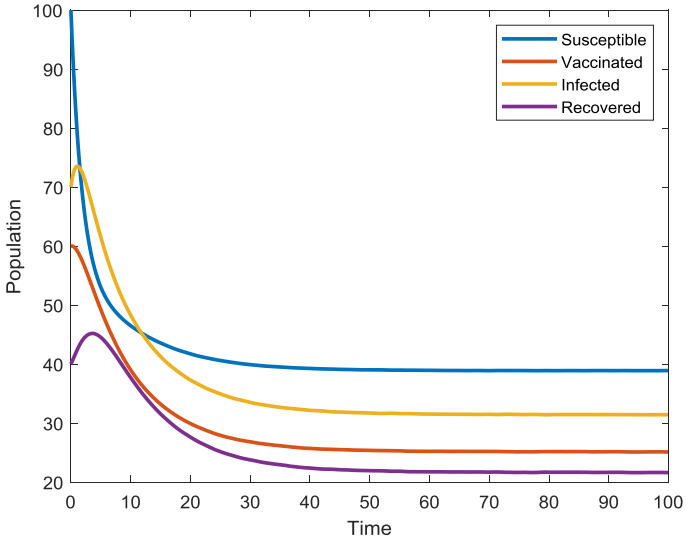

Figure 1(a) shows time series evaluation of population for the values of the attributes of example 1 with noise intensities $\alpha_1 = 0.01;\ \alpha_2 = 0.02;\ \alpha_3 = 0.01;\ \alpha_4 = 0.02$ and with initial values [100, 60, 70, 40].

Example 2 : $A = 12;\ \alpha = 0.15;\ \beta = 0.05;\ \gamma = 0.01;\ a = 2;\ b = 10;\ \theta = 0.2;\ \varepsilon = 0.2;\ \alpha_1 = 0.07;$ $\alpha_2 = 0.08;\ \alpha_3 = 0.07;\ \alpha_4 = 0.08$ with initial values [12, 10, 8, 5]

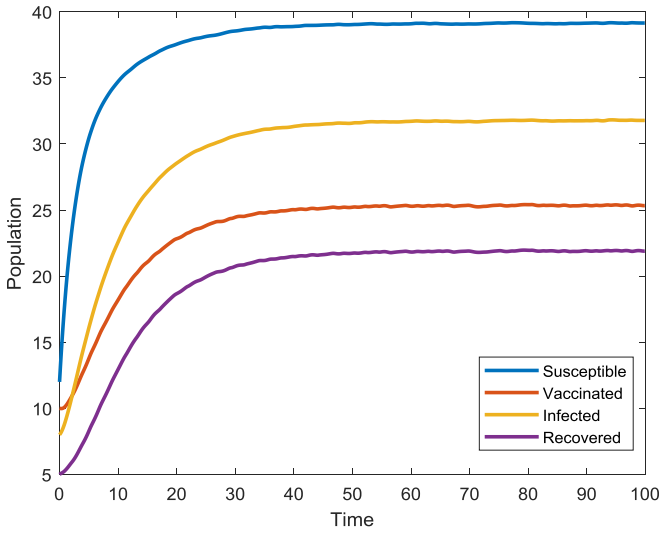

Figure 2

Figure 2 represents time series evaluation of population for the values of the attributes of example 2 with noise intensities $\alpha_1 = 0.07;\ \alpha_2 = 0.08;\ \alpha_3 = 0.07;\ \alpha_4 = 0.08;$ and with initial values [12, 10, 8, 5]

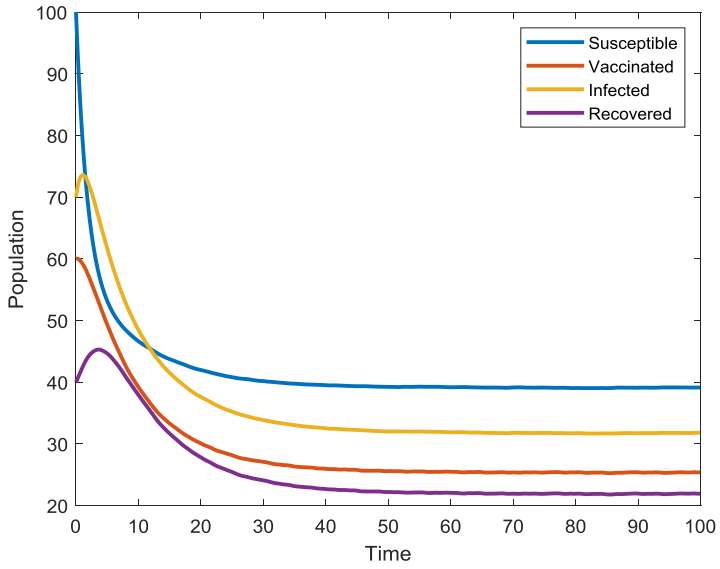

Figure 2(a)

Figure 2(a) represents time series evaluation of population for the values of the attributes of example 2 with noise intensities $\alpha_1 = 0.07;\ \alpha_2 = 0.08;\ \alpha_3 = 0.07;\ \alpha_4 = 0.08$ and with initial values [100, 60,70, 40]

Example 3: $A = 12;\ \alpha = 0.15;\ \beta = 0.05;\ \gamma = 0.01;\ a = 2;\ b = 10;\ \theta = 0.2;\ \varepsilon = 0.2;\ \alpha_1 = 1.5;$ $\alpha_2 = 1;\ \alpha_3 = 1.5;\ \alpha_4 = 1;$ with initial values [100, 60, 70, 40]

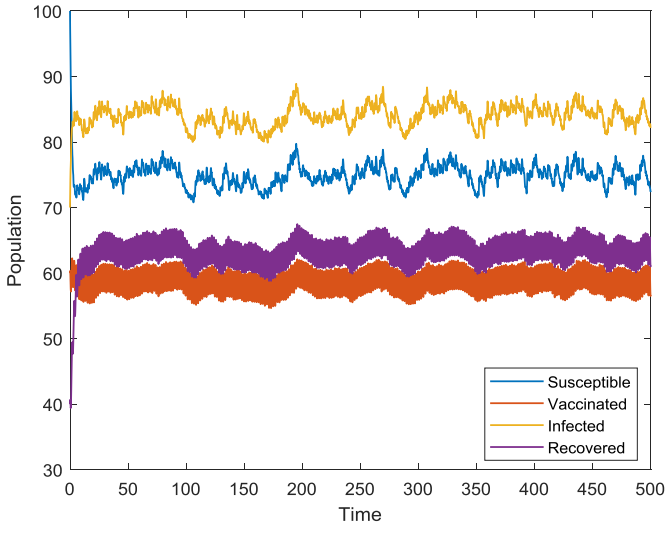

Figure 3

Figure 3 represents time series evaluation of population for the values of the attributes of example 3 with noise intensities $\alpha_1 = 1.5;\ \alpha_2 = 1;\ \alpha_3 = 1.5;\ \alpha_4 = 1$ and with initial values [100, 60,70, 40]

Example 4: $A=12;\ \alpha=0.15;\ \beta=0.05;\ \gamma=0.01;\ a=2;\ b=10;\ \theta=0.2;\ \varepsilon=0.2;\ \alpha_1=6;$ $\alpha_2=5;\ \alpha_3=6;\ \alpha_4=5$ with initial values [100, 60, 70, 40]

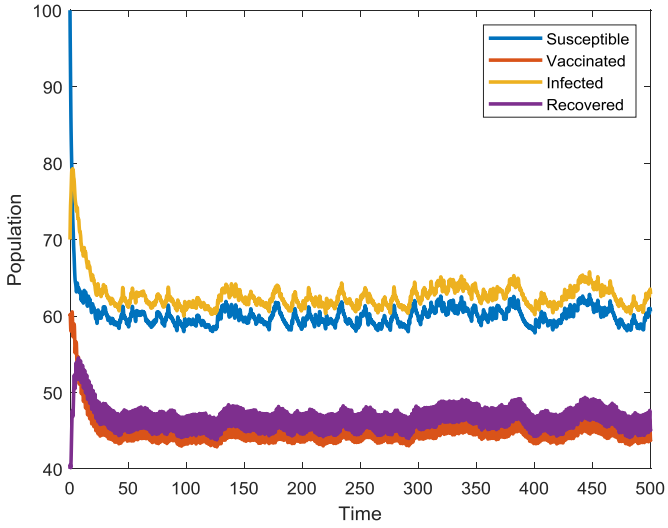

Figure 4

Figure 4 represents time series evaluation of population for the values of the attributes of example 4 with noise intensities $\alpha_1=6;\ \alpha_2=5;\ \alpha_3=6;\ \alpha_4=5$ and with initial values [100, 60, 70, 40]

Example 5: $A=12;\ \alpha=0.15;\ \beta=0.05;\ \gamma=0.01;\ a=2;\ b=10;\ \theta=0.2;\ \varepsilon=0.2;\ \alpha_1=10;$ $\alpha_2=8;\ \alpha_3=10;\ \alpha_4=8$ with initial values [100, 60, 70, 40]

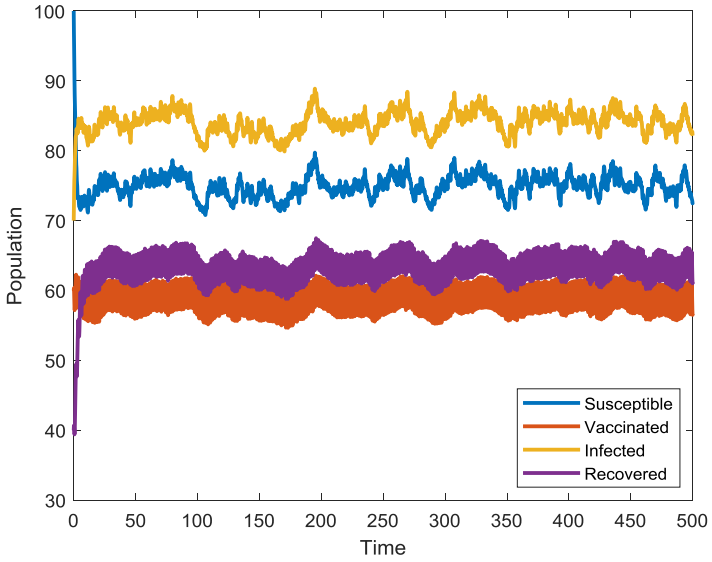

Figure 5

Figure 5 represents time series evaluation of population for the values of the attributes of example 5 with noise intensities $\alpha_1=10;\ \alpha_2=8;\ \alpha_3=10;\ \alpha_4=8$ and with initial values [100, 60, 70, 40]

Example 6 : $A=12;\ \alpha=0.15;\ \beta=0.05;\ \gamma=0.01;\ a=2;\ b=10;\ \theta=0.2;\ \varepsilon=0.2;\ \alpha_1=50;$ $\alpha_2=40;\ \alpha_3=50;\ \alpha_4=40$ with Initial Values [100;60;70;40]

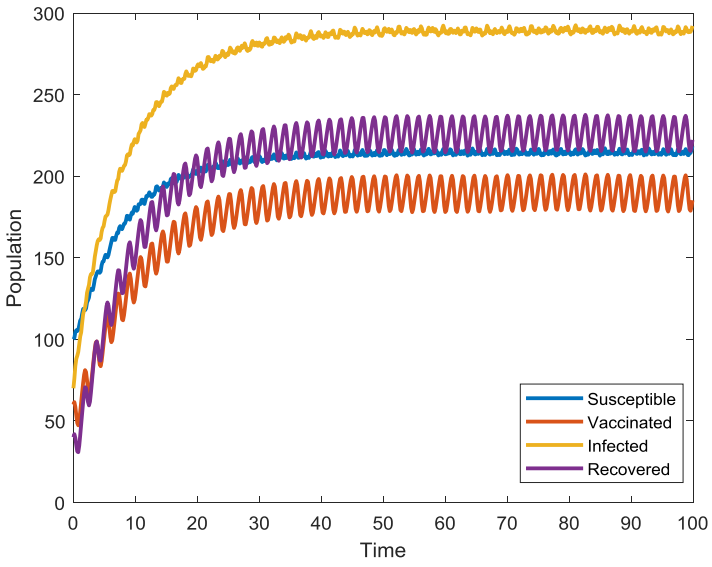

Figure 6

Figure 6 represents time series evaluation of population for the values of the attributes of example 6 with noise intensities $\alpha_1=50;\ \alpha_2=40;\ \alpha_3=50;\ \alpha_4=40$ and with initial values [100, 60, 70, 40]

Example 7 : $A=12;\ \alpha=0.15;\ \beta=0.05;\ \gamma=0.01;\ a=2;\ b=10;\ \theta=0.2;\ \varepsilon=0.2;\ \alpha_1=200;$ $\alpha_2=150;\ \alpha_3=200;\ \alpha_4=150$ with initial values [100; 60; 70; 40]

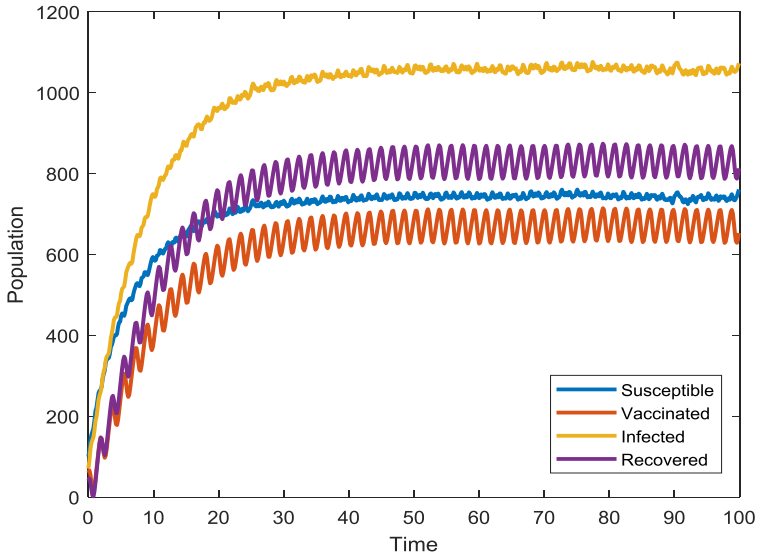

Figure 7

Figure 7 shows time series evaluation of population for the values of the attributes of example 7 with noise intensities $\alpha_1 = 200;\ \alpha_2 = 150;\ \alpha_3 = 200;\ \alpha_4 = 150$ and with initial values [100, 60, 70, 40]

6. Observations and remarks:

A model of an SVIR with noise was examined in this paper. Later, we looked at the impact of additive white noise on environmental variations near the positive equilibrium. MATLab is used to compute the population variances and examine them for stability. The numerical simulation and analytical results of the SVIR with noise system model reveal those population variances play a significant role in analysing the system's stability.

In a noisy environment, noise on the equation creates large oscillation variations around the equilibrium point, implying that our system is periodic. As observed in the pictures/graphs (1-7), numerical replications reveal that the system's trajectories oscillate arbitrarily with a wide range of amplitudes, with the strength of noises initially increasing but eventually oscillating.

As a result of the changes in responsive parameters, we conclude that stochastic perturbation causes a significant shift in the intensity of the dynamical scheme under discussion, resulting in massive environmental fluctuations.

7. Future scope:

In the SVIR mathematical model (2.1), we can add a diffusion term using the same notation (2.4). Analysing the dynamical properties of the model with diffusion and gaining insight into the regulation of stability in the presence of diffusion are critical. Increased diffusion coefficients can increase the potential for oscillatory behaviour and hence the corresponding results, according to the diffusion analysis.

References

1. Gumel AB, Mccluskey CC, Watmough J (2006) An SVEIR model for assessing the potential impact of an imperfect anti-SARS vaccine. Math Biosci Eng 3(3):485–512
2. Kumar A, Nilam (2018) Stability of a time delayed SIR epidemic model along with nonlinear incidence rate and Holling type II treatment rate. Int J Comput Methods 15(6):1850055
3. Kumar A, Nilam (2018) Dynamical model of epidemic along with time delay; Holling type II incidence rate and Monod–Haldane treatment rate. Differ Equ Dyn Syst To appear in volume 26(4). https://doi.org/10.1007/s12591-018-0424-8
4. Dubey B, Patara A, Srivastava PK, Dubey US (2013) Modelling and analysis of a SEIR model with different types of nonlinear treatment rates. J Biol Syst 21(3):1350023
5. Dubey B, Dubey P, Dubey US (2015) Dynamics of a SIR model with nonlinear incidence rate and treatment rate. Appl Appl Math 10(2):718–737

6. Hattaf K, Yousfi N (2009) Mathematical model of influenza A (H1N1) infection. Adv Stud Biol 1(8):383–390
7. Hattaf K, Lashari AA, Louartassi Y, Yousfi N (2013) A delayed SIR epidemic model with general incidence rate. Electron J Qual Theory Differ Equ 3:1–9
8. Zhou L, Fan M (2012) Dynamics of a SIR epidemic model with limited medical resources revisited. Nonlinear Anal 13(1):312–324
9. Alexander ME, Moghadas SM (2004) Periodicity in an epidemic model with a generalized nonlinear incidence. Math Biosci 189(1):75–96
10. Dubey P, Dubey B, Dubey US (2016) An SIR model with nonlinear incidence rate and Holling type III treatment rate. Appl Anal Biol Phys Sci 186:63–81
11. Xu R, Ma Z (2009) Stability of a delayed SIRS epidemic model with a nonlinear incidence rate. Chaos Solut Fractals 41(5):2319– 2325
12. Michael YL, Graef JR, Wang L, Karsai J (1999) Global dynamics of a SEIR model with varying total population size. Math Biosci 160(2):191–213
13. Zhang Z, Suo S (2010) Qualitative analysis of a SIR epidemic model with saturated treatment rate. J Appl Math Comput 34(1– 2):177–194
14. Hethcote HW (2000) The mathematics of infectious disease. SIAM Rev 42(4):599–653
15. Sarwardi S, Haque M, Mandal PK (2014) Persistence and global stability of Bazykin Predator Pray model with Beddington– DeAngelis response function. Commun Nonlinear Sci Numer Simul 19(1):189–209
16. 17. Liu WM, Hethcote HW, Levin SA (1987) Dynamical behavior of epidemiological models with nonlinear incidence rates. J Math Biol 25(4):359–380
17. 18. Shi X, Zhou X, Song X (2011) Analysis of a stage-structured predator-prey model with Crowley–Martin function. J Appl Math Comput 36(1–2):459–472
18. World health statistics. 2019, https://apps.who.int/iris/bitstream/h{and}le/10665/324835/9789241565707-eng.pdf?sequence=9&isAllowed=y accessed on 20, January 2021.
19. World health statistics. 2020, https://apps.who.int/iris/bitstream/h{and}le/10665/332070/9789240005105-eng.pdf, accessed on 20, 2021.
20. Hethcote HW, Driessche PVD. An SIS epidemicmodel with variable population size and a delay. J Math Biol 1995;34:177–94.
21. Zhou TT, Zhang WP, Lu QY. Bifurcation analysis of an SIS epidemic model with saturated incidence rate and saturated treatment function. Appl Math Comput 2014;226:288–305.
22. Kuniya T, Muroya Y. Global stability of a multi-group SIS epidemic model with varying total population size. Appl Math Comput 2015;265:785–98.
23. d'Onofrio A, Manfredi P, Salinelli E. Vaccinating behaviour, information, and the dynamics of SIR vaccine preventable diseases. Theor Popul Biol 2007;71:301–17.
24. Hattaf K, Lashari AA, Louartassi Y, Yousfi N. A delayed SIR epidemic model with general incidence rate. Electron J Qual Theory Differ Equ 2013;3:1–9.
25. Liu ZH, Yuan R. Zero-hopf bifurcation for an infection-age structured epidemic model with a nonlinear incidence rate. Sci China-Math 2017;60:1371–98.

26. Bai ZG, Wu SL. Traveling waves in a delayed SIR epidemic model with nonlinear incidence. Appl Math Comput 2015;263:221–32.
27. Kumar A, Goel K. Nilam, a deterministic time-delayed SIR epidemic model: mathematical modeling and analysis. Theory Biosci 2019;139:67–76.
28. Meng XZ, Wu ZT, Zhang TQ. The dynamics and therapeutic strategies of a SEIS epidemic model. Int J Biomath 2019;5:41–58.
29. Xu R, Zhang S, Zhang F. Global dynamics of a delayed SEIS infectious disease model with logistic growth and saturation incidence. Math Methods Appl Sci 2016;39:3294–308.
30. Huo HF, Yang P, Xiang H. Stability and bifurcation for an SEIS epidemic model with the impact of media. Physica A 2018;490:702–20.
31. Liu JM, Wei FY. Dynamics of stochastic SEIS epidemic model with varying population size. Physica A 2016;464:241–50.
32. Zhou XY, Cui JA. Analysis of stability and bifurcation for an SEIR epidemic model with saturated recovery rate. Commun Nonlinear Sci Numer Simul 2011;16:4438–50.
33. Krishnapriya P, Pitchaimani M, Witten TM. Mathematical analysis of an influenza a epidemic model with discrete delay. J Comput Appl Math 2017;324:155–72.
34. Khan MA, Khan Y, Islam S. Complex dynamics of an SEIR epidemic model with saturated incidence rate and treatment. Physica A 2018;493:210–27.
35. Wang LW, Zhang XA, Liu ZJ. An SEIR epidemic model with relapse and general nonlinear incidence rate with application to media impact. Qual Theory Dyn Syst 2018;17:309–29.
36. Fan XL, Wang L, Teng ZD. Global dynamics for a class of discrete SEIRS epidemic models with general nonlinear incidence. Adv Difference Equ 2016;123:1–20.
37. Jiang ZC, Ma WB, Wei JJ. Global Hopf bifurcation and permanence of a delayed SEIRS epidemic model. Math Comput Simulation 2016;122:35–54.
38. Jana S, Haldar P, Nandi SK, Kar TK. Global dynamics of a SEIRS epidemic model with saturated disease transmission rate and vaccination control. Int J Appl Comput Math 2017;3:43–64.
39. Cai LM, Li ZQ, Song XY. Global analysis of an epidemic model with vaccination. J Appl Math Comput 2018;57:605–28.
40. Zhang LW, Liu ZJ, Zhang XA. Global dynamics of an SVEIR epidemic model with distributed delay and nonlinear incidence. Appl Math Comput 2016;284:47–65.
41. Mathur KS, Narayan P. Dynamics of an SVEIRS epidemic model with vaccination and saturated incidence rate, Int J Appl Comput Math 4 (118) 1-22.
42. Zhao DL, Yuan SL. Persistence and stability of the disease-free equilibrium in a stochastic epidemic model with imperfect vaccine. Adv Difference Equ 2016;280:1–14.
43. Lan GJ, Chen ZW, Wei CJ, Zhang SW. Stationary distribution of a stochastic SIQR epidemic model with saturated incidence and degenerate diffusion. Physica A 2018;511:61–77.

44. Chen XY, Cao JD, Park JH, Qiu JL. Stability analysis and estimation of domain of attraction for the endemic equilibrium of an SEIQ epidemic model. Nonlinear Dynam 2017;87:975–85

45. Goel K, Kumar A. Nilam, A deterministic time-delayed SVIRS epidemic model with incidences and saturated treatment. J Eng Math 2020; 121:19–38.

46. Zhang, Z., & Upadhyay, R. K. (2021). Dynamical analysis for a deterministic SVIRS epidemic model with Holling type II incidence rate and multiple delays. Results in Physics, *24*, 104181.

47. Nisbet RM, Gurney WSC. Modelling fluctuating populations. New York: John Wiley; 1982.

48. Carletti M. Numerical simulation of a Campbell-like stochastic delay model for bacteriophage infection. An IMA J Mat Med Biol 2006; 23: 297–310.

49. Kalyan Das, M.N.Srinivas, M.A.S.Srinivas, N.H.Gazi, Chaotic dynamics of a three species prey-predator competition model with bionomic harvesting due to delayed environmental Noise as external driving force , C R Biologies- Elsevier, 335, 2012 , 503-513.

50. Kalyan Das, K. Shiva Reddy, M. N. Srinivas, N.H.Gazi, Chaotic dynamics of a three species prey–predator competition model with noise in ecology, Applied Mathematics and Computation (Elsevier), 231, 2014, 117-133.

51. Geetha, R., Madhusudanan, V. & Srinivas, M.N., Influence of Clamor on the Transmission of Worms in Remote Sensor Network, Wireless Pers Commun, 2021. https://doi.org/10.1007/s11277-020-08024-4.

52. Madhusudanan, V, Srinivas, M.N. & Sridhar, S. Effect of Noise on Pandemic Structure for Proliferation of Malevolent Nodes in Remote Sensor Network. Wireless Pers Commun, (2021). https://doi.org/10.1007/s11277-021-08224-6

53. M N Srinivas, V Madhusudanan, A V S N Murty, B. R. Tapas Bapu, A review article on wireless sensor networks in view of E-epidemic models, Wireless Personal Commun, April 5, 2021,. https://doi.org/10.1007/s11277-020-08024-4.